

1 **A 10-valent composite mRNA vaccine against both influenza and COVID-19**

2

3 Yang Wang^{1,2,#}, Qin Hai Ma^{1,#}, Man Li^{3,#}, Qianyi Mai¹, Lin Ma⁶, Hong Zhang³, Huiling Zhong³,
4 Nan Cheng⁶, Pei Feng⁴, Peikun Guan², Shengzhen Wu¹, Lu Zhang⁷, Jun Dai^{2,7,*}, Biliang Zhang^{3,5,*},
5 Weiqi Pan^{1,4,*}, Zifeng Yang^{1,2,4,*}

6

7 ¹ State Key Laboratory of Respiratory Disease, National Clinical Research Center for Respiratory
8 Disease, Guangzhou Institute of Respiratory Health, The First Affiliated Hospital of Guangzhou
9 Medical University, Guangzhou, 510000, China;

10 ² Guangzhou National Laboratory, Guangzhou, 510000, China;

11 ³ Argona Pharmaceuticals Co., Ltd., Guangzhou, 510000, China;

12 ⁴ Respiratory Disease AI Laboratory on Epidemic and Medical Big Data Instrument Applications,
13 Faculty of Innovation Engineering, Macau University of Science and Technology, Macau SAR,
14 999078, China;

15 ⁵ State Key Laboratory of Respiratory Disease, Laboratory of Computational Biomedicine,
16 Guangzhou Institutes of Biomedicine and Health, Chinese Academy of Sciences, Guangzhou
17 510000, China;

18 ⁶ Guangzhou RiboBio Co., Ltd, Guangzhou 510000, China;

19 ⁷ Technology Centre, Guangzhou Customs, Guangzhou 510000, China.

20

21 # These authors contributed equally to this work.

22 * Correspondence: jeffyah@163.com (Z.Y.); panweiqi@gird.cn (W.P.); bill.zhang@ribobio.com
23 (B.Z.); 19915302@qq.com (J.D.)

24

25 **Abstract**

26 The COVID-19 pandemic caused by SARS-CoV-2 viruses has had a persistent and significant
27 impact on global public health for four years. Recently, there has been a resurgence of seasonal
28 influenza transmission worldwide. The co-circulation of SARS-CoV-2 and seasonal influenza
29 viruses results in a dual burden on communities. Additionally, the pandemic potential of zoonotic
30 influenza viruses, such as avian Influenza A/H5N1 and A/H7N9, remains a concern. Therefore, a
31 combined vaccine against all these respiratory diseases is in urgent need. mRNA vaccines, with
32 their superior efficacy, speed in development, flexibility, and cost-effectiveness, offer a promising
33 solution for such infectious diseases and potential future pandemics. In this study, we present
34 FLUCOV-10, a novel 10-valent mRNA vaccine created from our proven platform. This vaccine
35 encodes hemagglutinin (HA) proteins from four seasonal influenza viruses and two avian
36 influenza viruses with pandemic potential, as well as spike proteins from four SARS-CoV-2
37 variants. A two-dose immunization with the FLUCOV-10 elicited robust immune responses in
38 mice, producing IgG antibodies, neutralizing antibodies, and antigen-specific cellular immune
39 responses against all the vaccine-matched viruses of influenza and SARS-CoV-2. Remarkably, the
40 FLUCOV-10 immunization provided complete protection in mouse models against both
41 homologous and heterologous strains of influenza and SARS-CoV-2. These results highlight the
42 potential of FLUCOV-10 as an effective vaccine candidate for the prevention of influenza and
43 COVID-19.

44

45 **Keywords:** mRNA vaccine, multi-valent, SARS-CoV-2, COVID-19, influenza

46

47

48 **Author summary**

49 Amidst the ongoing and emerging respiratory viral threats, particularly the concurrent and
50 sequential spread of SARS-CoV-2 and influenza, our research introduces FLUCOV-10. This
51 novel mRNA-based combination vaccine, designed to counteract both influenza and COVID-19,
52 by incorporating genes for surface glycoproteins from various influenza viruses and SARS-CoV-2
53 variants. This combination vaccine showed highly effective in preclinical trials, generating strong
54 immune responses, and ensuring protection against both matching and heterologous strains of
55 influenza and SARS-CoV-2. FLUCOV-10 represents a significant step forward in our ability to
56 address respiratory viral threats, showcasing potential as a singular, adaptable vaccine solution for
57 global health challenges.

58

59 Introduction

60 The coronavirus 2019 disease (COVID-19) pandemic, caused by the severe acute respiratory
61 syndrome coronavirus 2 (SARS-CoV-2), has had a substantial and multifaceted impact on global
62 public health over the past four years. As of 8 November 2023, the World Health Organization
63 (WHO) has documented 772 million confirmed cases and approximately 7.0 million cumulative
64 fatalities (1). These statistics, however, are likely to be underestimated, owing to a lack of
65 sufficient testing or poor reporting practices in the past years (2). Following a rigorous campaign
66 involving measures such as vaccinations, medications, and restrictions on social activities, the
67 COVID-19 pandemic has been brought under control. On 5 May 2023, the WHO lifted the status
68 of COVID-19 from a global emergency (3); nevertheless, this declaration does not imply that the
69 fight against infectious diseases has concluded. Numerous breakthrough infections with
70 SARS-CoV-2 among fully vaccinated individuals suggest the potential need for annual booster
71 vaccinations against COVID-19 (4).

72
73 Another major respiratory threat, seasonal influenza virus accounts for approximately one
74 billion cases each year, with 290,000 to 650,000 death globally (5, 6). A notable reduction in
75 influenza cases was observed during the 2020-2021 period, likely due to the widespread adoption
76 of nonpharmaceutical interventions during the COVID-19 pandemic. However, the subsequent
77 resurgence of influenza, occurring alongside SARS-CoV-2 and other respiratory diseases, has
78 presented a dual threat to global health systems (7). This scenario is complicated further by the
79 potential pandemic threat posed by zoonotic influenza viruses. While human infections with avian
80 and other zoonotic influenza viruses are relatively rare, they are considerably more lethal than
81 seasonal influenza, partly due to the absence of pre-existing immunity in the population (8, 9). For
82 example, the highly pathogenic avian influenza A/H5N1 virus has caused 878 cases with 458
83 fatalities (case fatality rate: 52.2%) since its first report in 1996, and the avian influenza A/H7N9
84 virus has led to 1568 cases with 616 deaths (39.3%) case fatality rate: since it first emerged in
85 2013 (10). The resurgence of influenza, the persistence of SARS-CoV-2, and the sporadic severity
86 of zoonotic influenza highlight the critical need for a comprehensive vaccination strategy.

87
88 In the realm of vaccine strategies, mRNA-based platforms have been distinguished by their
89 satisfactory safety profile, high efficacy, adaptability, swift production timelines, and relatively
90 low manufacturing costs (11, 12). Amid the COVID-19 pandemic, mRNA vaccines encoding the
91 SARS-CoV-2 spike protein, not only received their initial authorization for human use but also
92 rapidly became the most widely used globally, credited to their potent efficacy and expedited
93 development timelines (13-15). However, the vaccines faced reduced effectiveness with the
94 emergence of omicron variant (16, 17). Consequently, the mRNA vaccines were promptly adapted
95 to include bivalent components, targeting both the ancestral and the omicron strain, and
96 demonstrated a superior neutralizing antibody response against omicron compared to the original
97 mRNA vaccines (18-22). The flexibility of the mRNA vaccine platform is further demonstrated by
98 its adaptability to other respiratory diseases; for instance, mRNA-LNP vaccines encoding the HA
99 proteins of avian influenza H10N8 and H7N9 have been shown to be highly immunogenic in
100 phase 1 clinical trials (23), while a quadrivalent mRNA vaccine for seasonal influenza has
101 displayed moderate to high immunogenicity in trials spanning phases 1 to 3 (24, 25).

102

103 In this study, we leveraged our established mRNA-LNP vaccine platform (11, 12) to create a
104 novel 10-valent mRNA vaccine, aimed at targeting a diverse spectrum of respiratory pathogens.
105 This vaccine is composed of components for all four seasonal influenza viruses (A/H1N1pdm09,
106 A/H3N2, B/Victoria, B/Yamagata), two avian influenza viruses with pandemic potential (A/H5N1
107 and A/H7N9), and four strains of SARS-CoV-2 (Wuhan-Hu-1, BQ.1.1, BA.2.75.2, XBB.1.5).
108 Subsequently, we evaluated the *in vitro* protein expression of this mRNA-based vaccine and
109 confirmed its immunogenicity in mice. Moreover, we demonstrated its effectiveness in providing
110 protection against infections from both COVID-19 and influenza.

111

112 **Results**

113 **Design and characterization of the 10-valent mRNA vaccine (FLUCOV-10)**

114 We developed a 10-valent mRNA vaccine candidate, named FLUCOV-10, which is designed to
115 provide broad protection against a wide range of influenza and SARS-CoV-2 viruses (Figure 1A).
116 The FLUCOV-10 comprises mRNAs encoding full-length HAs of each component of the
117 quadrivalent influenza vaccines for use in the 2022-2023 influenza season in the Northern
118 Hemisphere (i.e., A/Wisconsin/588/2019 (H1N1) pdm09, A/Darwin/6/2021 (H3N2),
119 B/Austria/1359417/2021, and B/Phuket/3073/2013), and the HAs of two avian influenza viruses
120 posing potential pandemic risks (i.e., A/Thailand/NBL1/2006 (H5N1) and
121 A/Anhui/DEWH72-03/2013 (H7N9)). The HA protein was selected for the influenza component
122 due to its role as a target for neutralizing antibodies and its key function in viral entry (6). The
123 FLUCOV-10 also includes mRNAs encoding the full-length spike proteins of ancestral
124 SARS-CoV-2 virus and three omicron variants (i.e., BQ.1.1, BA.2.75.2, and XBB.1.5).

125

126 To contextualize the sequences of vaccine strains, we conducted phylogenetic analysis using all
127 the available HA gene sequences of influenza A/H1N1, A/H3N2, A/H5N1, A/H7N9, B/Yamagata,
128 and B/Victoria collected since 2000, as well as all available SARS-CoV-2 spike genes (Figure 1B
129 and C). The vaccine strains for seasonal influenza in FLUCOV-10 were selected to represent the
130 currently circulating strains (Figure 1B), while the vaccine strains for avian influenza viruses were
131 chosen based on the WHO's recommendations for vaccine candidates (26). In FLUCOV-10, the
132 inclusion of the ancestral SARS-CoV-2 strain is designed to offer cross-protection against several
133 variants of concern, such as alpha, beta, gamma, delta and so on (11). Additionally, the
134 incorporation of three Omicron subvariants in FLUCOV-10 was deliberately designed to address
135 the newly emerged circulating SARS-CoV-2 variants, which possess escape properties to
136 neutralization (27, 28) (Figure 1C).

137

138 To assess the *in vitro* expression profile of each component in FLUCOV-10, western-blotting
139 was performed using HA- or spike-specific antibodies. As anticipated, cell lysates from the
140 mRNA-transfected HEK293T cells exhibited a high expression level of each component (Figure
141 1D and E). Among the FLUCOV-10 expressing HAs, five (i.e., A/H1, A/H3, A/H7, B/Yamagata,
142 and B/Victoria) were expressed in their precursor form (HA0), while A/H5 was present in both its
143 precursor and cleaved forms (HA1 and HA2) (Figure 1D). This is due to the multibasic amino
144 acid motif at the cleavage site of A/H5, which is more susceptible to cellular cleavage (29, 30). All

145 the expressed spike proteins were maintained in their full-length form due to the intentional
146 removal of both the furin-like cleavage motif and the S2 cleavage motif (Figure 1 E).

147

148 After encapsulating the mRNA into lipid nanoparticles (LNP), we assessed the particle size of
149 each component in FLUCOV-10. The measurements revealed that each mRNA-LNP component
150 consistently displayed similar average particle sizes, ranging from 90.7 to 103.9 nm (Figure 1F).

151

152 **FLUCOV-10 elicits a robust humoral immune response in BALB/c mice**

153 To evaluate the immunogenicity of FLUCOV-10, we intramuscularly administered two doses of
154 the vaccine to 6-8-week-old BALB/c mice, with a three-week interval between doses. Each dose
155 contained 50 µg of mRNA, which includes 5 µg of each individual mRNA. A control group of
156 animals was injected with a placebo. At 14 days post-booster immunization, serum samples were
157 collected, and HA- or spike-specific antibody responses were determined by ELISA and
158 micro-neutralization assays. The results showed that compared to placebo group, mice immunized
159 with FLUCOV-10 produced 5,161-131,072-fold higher IgG antibody titers against all the 10
160 encoded HAs or spikes ($p < 0.0001$) (Figure 2A and B). In addition, the FLUCOV-10 vaccine
161 elicited neutralizing antibodies against all the vaccine matched influenza viruses and
162 SARS-CoV-2 viruses; whereas placebo did not induce detectable neutralizing antibodies against
163 any of these viruses (Figure 2C and D). Intriguingly, the FLUCOV-10 induced varying levels of
164 neutralizing antibody titers against different influenza viruses, with titers ranging from 202 to
165 12,902 (Figure 2C). The neutralizing antibody titers against B/Yamagata and B/Victoria were at
166 lower levels compared to those against other influenza or SARS-CoV-2 viruses, reflecting the
167 trend observed in their IgG titers (Figure 2A).

168

169 To explore the reason of the varied antibody responses, we simultaneously administered 5 µg
170 doses of monovalent mRNA-LNP formulations for each component of FLUCOV-10, to BALB/c
171 mice using the same vaccination regime. Monovalent mRNA-LNP vaccines induced neutralizing
172 antibody titers were also at lower levels against B/Yamagata and B/Victoria compared to those
173 against other influenza viruses (Figure 2C). Moreover, A/H5N1, B/Yamgata, and B/Victoria
174 neutralizing antibodies were 3.5~6.3-fold lower in mice receiving the FLUCOV-10 vaccine
175 compared with those receiving A/H5N1, B/Yamgata, and B/Victoria mRNA-LNPs, respectively (p
176 = 0.0148, $p < 0.0001$, and $p < 0.0001$, respectively). These findings indicate that the mRNA-LNP
177 of B/Yamaga and B/Victoria exhibited low immunogenicity and their immunogenicity was further
178 attenuated by the presence of other components in the multivalent mRNA vaccine formulation.

179

180 In summary, two immunizations with FLUCOV-10 effectively elicited antibody responses
181 against influenza and SARS-CoV-2 viruses.

182

183 **FLUCOV-10 elicits an antigen-specific Th1 cellular immune response in BALB/c mice**

184 To assess the activation of HA- and spike-specific cellular immunity, we determined the
185 antigen-specific cytokine producing splenocytes in vaccinated mice at 14 days post booster
186 immunization by ELISpot. The results showed that the FLUCOV-10 elicited significantly higher
187 HA- and spike-specific interferon γ (IFN- γ) and interleukin-2 (IL-2) producing splenocytes,
188 compared to those of placebo (Figure 3A and B), while the FLUCOV-10 did not elicit higher IL-4

189 and IL-5 producing splenocytes (Figure 3C and D). These results indicate that the FLUCOV-10
190 vaccination activates Th1-biased immune responses, aligning with the observation in our
191 previously developed mRNA vaccine platform (11, 12).

192

193 Of interest, the splenocytes producing IFN- γ and IL-2 in response to FLUCOV-10 vaccination
194 showed varying levels when stimulated with different antigens. Among the influenza HAs,
195 A/H3-specific IFN- γ and IL-2 secreting cells reached the highest level, while those specific to
196 B/Victoria reached the lowest level (Figure 3A and B). These results correlate with the trend
197 observed in the subtype-specific HA IgG antibody and neutralizing antibody responses (Figure 2A
198 and C).

199 **FLUCOV-10 protects mice from homologous and heterologous challenge with influenza** 200 **viruses**

201 To explore the protection efficacy against antigenically similar or heterologous influenza
202 viruses, BALB/c mice immunized with two doses of FLUCOV-10 or placebo were challenged
203 intranasally with A/California/04/09 (H1N1), rgA/Guangdong/17SF003/2016 (H7N9), or
204 B/Florida/4/2006 (Yamagata lineage) three weeks after the final immunization and monitored for
205 their weight loss and survival daily (Figure 4A). The rgA/Guangdong/17SF003/2016 (H7N9)
206 strain was antigenically similar with the A/H7 components in FLUCOV-10 (31, 32). In contrast,
207 the A/California/04/09 (H1N1) and B/Florida/4/2006 were both genetically and antigenically
208 distinct from the corresponding components of FLUCOV-10, as the significant different
209 neutralizing antibody titers were observed when comparing vaccine-matched viruses and the
210 challenge viruses to the same mouse sera (i.e., anti-A/Victoria/2570/2019 versus
211 anti-A/California/04/09; anti- B/Phuket/3073/2013 versus B/Florida/4/2006) (Figure 1C and
212 Supplemental Figure 1).

213

214 Mice immunized with the FLUCOV-10 showed significantly less weight loss than mice
215 immunized with the placebo ($p < 0.01$) against challenge by either antigenically matched
216 (rgA/H7N9) or heterologous virus (A/H1N1 and B/Yamagata) (Figure 4B, E, and H). Remarkably,
217 while no survival was observed in the placebo-treated groups, the mice receiving FLUCOV-10
218 were completely protected against both vaccine-matched and heterologous viral challenges
219 (Supplemental Figure 2A-C). To assess viral loads in upper and lower respiratory tract, mice were
220 sacrificed 3 and 6 days after challenge, and lung and nasal turbinate tissues were collected for
221 determination of viral loads by TCID50. Mice in the FLUCOV-10 groups exhibited no detectable
222 virus in their turbinate or lung tissues at both 3 and 6 days following the challenge with either of
223 the viruses, whereas mice from corresponding placebo groups showed significantly higher viral
224 loads in both turbinate and lung tissues (Figure 4C, F, and I). To observe pulmonary lesions and
225 inflammation, lung tissues at 3 and 6 days post challenge were collected for sectioning and
226 staining. Mice from the placebo groups exhibited extensive pulmonary lesions and inflammation
227 at both 3 and 6 days post-challenge with all three viruses (Figure 4D, G, and J). In contrast, mice
228 immunized with FLUCOV-10 showed either mild or no apparent pulmonary lesions and
229 inflammation following challenges with any of the viruses.

230

231 In summary, FLUCOV-10 provides complete protection against both homologous and
232 heterologous influenza viruses, effectively preventing viral replication, lung lesions, and

233 inflammation in the respiratory tract.

234

235 **FLUCOV-10 protects mice from challenge with SARS-CoV-2 viruses**

236 To determine the protection efficacy against homologous and heterologous SARS-CoV-2
237 viruses, K18-hACE2 mice immunized with two doses of FLUCOV-10 or placebo were challenged
238 intranasally with $10^{4.5}$ TCID₅₀ of XBB.1.5 and 10^4 TCID₅₀ of BA.5.2, respectively (Figure 5A).
239 The XBB.1.5 strain belongs to the same clade as the vaccine component included in FLUCOV-10.
240 In contrast, the BA.5.2 subvariant is not incorporated in the FLUCOV-10 vaccine formulation.
241 (Figure 1C).

242

243 Mice immunized with the FLUCOV-10 showed significantly less weight loss than mice
244 immunized with the placebo against XBB.1.5 and BA.5.2 challenge ($p = 0.0009$ and $p = 0.0128$,
245 respectively, at 5 days post challenge) (Figure 4B, E, and H). Of note, while no mice from placebo
246 groups survived after either XBB.1.5 or BA.5.2 strain challenge, the mice receiving FLUCOV-10
247 were completely protected against both XBB.1.5 and BA.5.2 virus challenges (Supplemental
248 Figure 2E and F). To assess viral loads in respiratory tract, mice were sacrificed 3 and 6 days after
249 challenge, and lungs were collected for determination of viral loads by TCID₅₀. Mice in the
250 FLUCOV-10 groups exhibited no detectable virus in their lungs at both 3 and 6 days post
251 challenge with either of the viruses, whereas mice from corresponding placebo groups showed
252 significantly higher viral loads (Figure 4C, F, and I). Pulmonary lesions and inflammation were
253 determined at 3 and 6 days post challenge. Mice from the placebo groups exhibited moderate to
254 severe pulmonary lesions and inflammation at both 3 and 6 days post-challenge with both viruses
255 (Figure 4D, G, and J). In contrast, mice immunized with FLUCOV-10 did not show apparent
256 pulmonary lesions and inflammation following challenges with either of the viruses.

257

258 In summary, FLUCOV-10 provides complete protection against both homologous and
259 heterologous SARS-CoV-2 viruses, effectively preventing viral replication, lung lesions, and
260 inflammation in the respiratory tract.

261

262 **Discussion**

263 Given the simultaneous and consecutive circulation of SARS-CoV-2 and seasonal influenza
264 viruses, coupled with the looming threat posed by zoonotic influenza viruses, there is a
265 pronounced and urgent need for the development of a combination vaccine targeting both
266 SARS-CoV-2 and influenza viruses. Recently, various research groups have developed
267 combination vaccines by using inactivated (33), recombinant protein (34, 35), and mRNA
268 platforms (36-38). In the present study, we have utilized our previously established mRNA
269 vaccine platform to design and assess FLUCOV-10, a universal vaccine that targets a broader
270 range of distinct SARS-CoV-2 and influenza viruses. This vaccine comprises decavalent mRNAs
271 encoding the full-length HAs of all four seasonal influenza viruses and two avian influenza viruses,
272 as well as the full-length spikes of four different SARS-CoV-2 strains. This composition allows
273 FLUCOV-10 to provide extensive protection against a wide spectrum of these respiratory viruses.
274 To the best of our knowledge, FLUCOV-10 represents the first vaccine candidate that
275 simultaneously targets SARS-CoV-2, seasonal, and avian influenza.

276

277 Ensuring the immunogenicity and efficacy of each component is a fundamental challenge in the
278 development of combination vaccines (39). The FLUCOV-10 vaccine addresses this by
279 incorporating 5 µg of each mRNA component, based on our previous reports showing that two
280 doses of 5 µg in monovalent or bivalent mRNA vaccines achieved sterilizing immunity in mice, an
281 effect comparable to a 20 µg dose (11, 12). We dissected the protein expression and immune
282 response induction for each component of FLUCOV-10. Similar to previous findings (11, 12),
283 each component in FLUCOV-10 resulted in abundant expression of HA or spike proteins in cell
284 lysates (Figure 1 D and E), leading to robust component-specific humoral responses (Figure 2)
285 and Th1-favored cellular responses (Figure 3) following a two-dose regimen. In response to the
286 constantly evolving and antigenically diverse strains of influenza and SARS-CoV-2, we also
287 evaluated the cross-reactive immunity conferred by FLUCOV-10. Our findings revealed that
288 FLUCOV-10 produces strong neutralizing antibodies against antigenically distinct influenza
289 viruses and inter-sublineage variants of SARS-CoV-2 (Supplemental Figure 1), surpassing known
290 surrogate correlates of protection (40, 41). In line with expectations, animal challenge studies
291 showed that FLUCOV-10 provided complete protection to immunized mice against both
292 homologous and heterologous challenges of influenza and SARS-CoV-2 viruses, evidenced by
293 significantly less body weight loss, 100% survival rates, undetectable viral loads in the respiratory
294 tract, and absence of pulmonary lesions and inflammation. These findings suggest that
295 FLUCOV-10 is a promising candidate vaccine, effectively targeting SARS-CoV-2, seasonal
296 influenza, and avian influenza viruses simultaneously.

297

298 The full-length membrane-bound HA surface glycoprotein was selected for the influenza
299 component of FLUCOV-10 due to its high immunogenicity and ability to elicit both
300 strain-specific and cross-reactive immune responses (42, 43). Interestingly, we observed varying
301 levels of immunogenicity among the different influenza HA components. Notably, the two mRNA
302 components corresponding to influenza B viruses showed relatively low immunogenicity, as
303 evidenced by their production of lower levels of IgG antibodies, neutralizing antibodies, and
304 IFN-γ and IL-2 secreting lymphocytes, compared to those of other HA components. Observations
305 from licensed influenza vaccines and a quadrivalent seasonal influenza mRNA vaccine candidate
306 showed a similar pattern of lower influenza B strain responses (24, 44, 45). Upon further
307 examination, we found that monovalent mRNA vaccines for both influenza B lineages generated
308 significantly lower neutralizing antibodies than those for influenza A subtypes. Notably, the
309 influenza B mRNA components in FLUCOV-10 produced even lower antibody levels compared
310 to their monovalent counterparts. These results suggest that the reduced efficacy of influenza B
311 components in FLUCOV-10 arises from both intrinsic factors and interactions within the other
312 components of the vaccine. This observation warrants further investigation into optimizing the
313 balance of components in multivalent vaccines.

314

315 The goal of a combined mRNA vaccine is to provide robust immunization across as many
316 components as possible. Arevalo et al. reported a promising universal influenza mRNA vaccine
317 comprising 20 HAs from 18 influenza A subtypes and 2 influenza B lineages (46). However, their
318 study revealed that mice immunized with this 20-HA mRNA vaccine (2.5 µg per component)
319 suffered a body weight loss of over 10% after being challenged with 5LD₅₀ of A/California/7/2009

320 (H1N1pdm). In contrast, in the current study, mice vaccinated with FLUCOV-10 (5 µg per
321 component) did not show obvious weight loss when challenged with 10LD₅₀ of a comparable
322 virus. This underscores the need for strategic adjustments in the number and dosage of
323 components in combined mRNA vaccines to achieve maximum efficacy.

324

325 For the development of multivalent or combined mRNA vaccines, encapsulating each mRNA
326 encoding separate antigens is a common approach, despite the efficiency of encapsulating all
327 mRNAs simultaneously (36, 46-48). This method of individual LNP preparation facilitates the
328 convenient verification of each mRNA vaccine component's qualification, concentration, and
329 immunogenicity (46). Additionally, in the case of combined vaccines where one component is
330 already marketed and another is developed subsequently, it is generally necessary to manufacture
331 each mRNA-LNP separately (47).

332

333 COVID-19 and influenza share challenges related to viral evolution and a decline in vaccine
334 protection over time (49-52). Both diseases also exhibit seasonal trends (53), underscoring the
335 potential need for annual booster vaccinations. Our FLUCOV-10 vaccine offers a flexible solution
336 to these challenges, capable of swiftly adapting to emerging strains. This allows for an annual
337 update of vaccine components to effectively combat newly emerging mutants or variants. The
338 combination vaccine approach of FLUCOV-10 also streamlines immunization, reducing the
339 number of injections, enhancing compliance, and minimizing adverse reactions (54, 55). This
340 efficiency saves time for families and reduces healthcare visits, easing the burden on both
341 individuals and healthcare systems. However, a critical aspect to consider is the phenomenon
342 observed with repeated influenza vaccinations, where a blunted immune response and reduced
343 vaccine effectiveness have been documented over time (56, 57). This observation highlights a
344 critical consideration for future combination vaccine strategies involving COVID-19: the
345 possibility that administering repeated COVID-19 vaccinations in a combination vaccine format
346 might lead to diminishing immunogenicity. Consequently, further research is crucial to validate
347 this hypothesis and develop and refine combination vaccine strategies to effectively tackle these
348 dynamic and evolving viral threats.

349

350 In conclusion, our study highlights the feasibility and efficacy of a broad-spectrum mRNA
351 vaccine, FLUCOV-10, in addressing the complex landscape of respiratory viral threats.
352 Furthermore, the FLUCOV-10 vaccine offers a versatile and potentially effective tool in the global
353 effort to control and prevent respiratory viral diseases. These findings underscore the value of
354 continuing research and translation into clinical practice to establish the real-world efficacy and
355 applicability of this vaccine approach.

356

357 **Materials and methods**

358 **Cells**

359 MDCK cells (CCL-34, American Type Culture Collection [ATCC]), human embryonic kidney
360 293T cells (CRL-3216, ATCC), and Vero E6 cells (CRL-1586, ATCC) were cultured in
361 Dulbecco's Modified Eagle medium (DMEM, Gibco) supplemented with 10% fetal bovine serum
362 (FBS) at 37°C with 5% CO₂.

363 **Viruses**

364 Recombinant influenza viruses containing HA and NA from
365 A/Victoria/2570/2019(H1N1)pdm09 (GISAID accession No., EPI1804971 and EPI1804972,
366 respectively), HA and NA from A/Darwin/6/2021(H3N2) (GISAID accession No., EPI1998552
367 and EPI1998553, respectively), and HA and NA from B/Austria/1359417/2021(Victoria lineage)
368 (GISAID accession No., EPI1921345, and EPI1921346, respectively) were created in the genetic
369 background of A/Puerto Rico/8/34 (PR8) or B/Lee/40 as previously described (31). The
370 recombinant H5N1 influenza virus containing the HA and NA genes derived from
371 A/Vietnam/1194/2004(H5N1) and the recombinant H7N9 influenza viruses containing the HA and
372 NA genes derived from A/Anhui/1/2013(H7N9) or A/Guangdong/17SF003/2016(H7N9) were
373 constructed previously in our laboratory (31, 32, 58). The A/California/04/2009(H1N1) was kindly
374 provided by Yi Shi (Chinese Academy of Sciences), the B/Florida/4/2006(Yamagata lineage) was
375 kindly provided by Jingxian Zhao (Guangzhou Medical University), and the B/Phuket/3073/2013
376 (Yamagata lineage) was obtained from National Institute for Biological Standards and Control
377 (NIBSC). All the influenza viruses were confirmed by sanger sequencing and propagated in
378 10-day-old embryonated eggs.

379 The SARS-CoV-2 viruses, including Wuhan-hu-1 (WH), BQ.1.1, BA.2.75.2, XBB.1.5, BA.5.2,
380 were isolated from COVID-19 patients and were propagated in Vero E6 cells. All experiments
381 involving these authentic SARS-CoV-2 strains were carried out in the BSL-3 Laboratory of the
382 Guangzhou Customs District Technology Center.

383 **mRNA synthesis**

384 The sequences encoding full-length spike proteins of SARS-CoV-2 viruses and the sequences
385 encoding full-length HAs of influenza viruses were human codon optimized and cloned into a
386 plasmid vector with the T7 promoter, 5' and 3' untranslated regions (UTRs) (59, 60), and a 120nt
387 poly-A tail (61). To improve the spike protein's stability and reduce protease cleavage, 2P
388 mutations (K986P/V987P), furin cleavage site mutations (RRAR to GGSG), and S2' cleavage site
389 mutations (KR to AN) were introduced into its encoding sequences as described previously (11).
390 The mRNAs were synthesized *in vitro* by T7 polymerase mediated transcription where the
391 uridine-5'-triphosphate (UTP) was substituted with pseudouridine-5'-triphosphate (pseudo-UTP).
392 Capped mRNAs were generated by supplementing the transcription reactions with RIBO-Cap4.
393 mRNA was purified by reversed-phase high-performance liquid chromatography (RP-HPLC) (62).
394 RNA quality was analyzed by bioanalyzer analysis (Agilent 2200 Tape station). mRNA
395 concentrations were measured by UV spectroscopy.

396 DNA sequences synthesized for this study originated from the following list of spike proteins
397 and HAs that were included: Wuhan-Hu-1 (GenBank accession No. 43740568),
398 hCoV-19/Switzerland/TI-EOC-38005531/2022 (BQ.1.1, GenBank accession No. OX366792.2),
399 hCoV-19/England/PHEC-YY8HAYE/2023 (BA.2.75.2, GISAID accession No.
400 EPI_ISL_16679125), hCoV-19/USA/CT-YNH-2509/2023 (XBB.1.5, GISAID accession No.
401 EPI_ISL_16570202), A/Wisconsin/588/2019 (H1N1)pdm09 (GISAID accession No.
402 EPI_ISL_404460), A/Darwin/6/2021(H3N2) (GISAID accession No. EPI_ISL_2233238),
403 A/Thailand/NBL1/2006 (H5N1) (GenBank accession No. KJ907470:1-1707),
404 A/Anhui/DEWH72-03/2013 (H7N9) (GenBank accession No. CY181529:22-1704),
405 B/Austria/1359417/2021 (B/Victoria lineage) (GISAID accession No. EPI_ISL_2378894),
406 B/Phuket/3073/2013 (B/Yamagata lineage) (GISAID accession No. EPI_ISL_161843).

407 **mRNA-LNP preparations**

408 The FLUCOV-10 vaccine comprises a total of 50 µg of mRNA, distributed equally among 10
409 different mRNAs (5 µg each). These mRNAs encode the HA and spike antigens from six influenza
410 viruses and four SARS-CoV-2 viruses, as detailed above. Each mRNA is separately formulated
411 into Lipid nanoparticles (LNPs) and then mixed, prior to vialing so 10 different mRNA
412 formulations are present in the vial. LNPs were prepared by microfluidic mixing using the
413 previously described method (63). Briefly, lipids were dissolved in ethanol at molar ratios of
414 45:16:15:1.0 (Ionizable lipid: Cholesterol: DSPC: DMG-PEG2000). The lipid mixture was rapidly
415 combined with a buffer of 50 mM sodium citrate (pH 4.0) containing mRNA at a volume ratio of
416 aqueous: ethanol using a microfluidic mixer (PNI Nanosystems, Vancouver, BC, Canada).
417 Formulations were dialyzed against PBS (pH 7.2) in the dialysis cassettes (Thermo Scientific,
418 Rockford, IL, USA) for at least 18 h. Formulations were diluted with PBS (pH 7.2) to reach a
419 required concentration, and then passed through a 0.22-mm filter and stored at 4°C until use.
420 Formulations were analyzed for particle size by using a ZETASIZER, and the mRNA
421 encapsulation, residues, endotoxin and bioburdens were also confirmed.

422 **mRNA transfection**

423 293T cells were seeded in 12-well plates at 1×10^6 cells per well and cultured at 37 °C in 5%
424 CO₂ for 16 h. 10 µg of each mRNA encoding HA or spike protein was transfected into 293T cells
425 using riboFECTTmRNAtransfection Reagent (C11055, Ribobio, Guangzhou, China). Cell
426 lysates were harvested by RIPA lysis buffer (R0030, Solarbio, Beijing, China) at 48 h after
427 transfection, and mixed with 5 × SDS-loading, following by centrifugation at 12,000 × g. The
428 samples were loaded for SDS-PAGE. The HA and spike proteins in cell lysates were then detected
429 by western blotting using a mouse monoclonal antibody against SARS-CoV-2 spike proteins
430 (GTX632604, GeneTex), a rabbit polyclonal antibody against influenza A/H1 HA (11055-T62,
431 Sino Biological), a mouse monoclonal antibody against influenza A/H3 HA (11056-MM03, Sino
432 Biological), a rabbit polyclonal antibody against influenza A/H5 HA (11062-T62, Sino
433 Biological)], a rabbit polyclonal antibody against influenza A/H7 HA (40103-T62, Sino
434 Biological) a rabbit polyclonal antibody against influenza B/Yamagata lineage HA (11053-T62,
435 Sino Biological), and a mouse monoclonal antibody against Influenza B/Victoria lineage HA
436 (11053-MM06, Sino Biological). β-actin was detected using anti-β-actin antibody.

437 **Animal experiments.**

438 BALB/c mouse experiments were performed in accord with Regulations of Guangdong
439 Province on the Administration of Laboratory Animals and Institutional Animal Care and Use
440 Committee of Guangzhou Medical University (IACUC Approval No. IACUC-2023-001). Six- to
441 eight-week-old female BALB/c mice (Guangdong Vital River Laboratory Animal Technology,
442 Guangzhou, China) were immunized intramuscularly with 5 µg of each monovalent mRNA-LNP
443 (in a 50 µl volume), 50 µg of FLUCOV-10 (in a 50 µl volume) or an equal volume of placebo and
444 boosted with an equal dose at 21 days post-initial immunization. Serum samples were collected
445 prior to initial immunization and 14 days after booster immunization. For influenza virus
446 challenges, vaccinated mice were anesthetized and infected intranasally with 10LD₅₀
447 A/California/07/2009 (H1N1), 10LD₅₀ of recombinant A/Guangdong/17SF003/2016 (H7N9)
448 (referred to as rgA/Guangdong/17SF003/2016 H7N9)), or 3 LD₅₀ of B/Florida/4/2006 in 50 µl of
449 PBS at 3 weeks after booster immunization. Weight loss and survival were monitored for 14 days
450 after challenge. Animals that lost more than 25% of their initial body weight were humanely

451 anesthetized. At 3 and 6 days post challenge, mouse lungs and nasal turbinates were collected for
452 viral titration and histological analyses.

453 For SARS-CoV-2 challenges, six- to nine-week-old female K18-hACE2 mice (Gempharmatech,
454 Nanjing, China) were immunized with the same regimen as that of BALB/c mouse experiments.
455 Three weeks post booster immunization, the mice were infected intranasally with 10^4 TCID₅₀ of
456 hCoV-19/Uganda/UG1282/2022 (BA.5.2) or $10^{4.5}$ TCID₅₀ of hCoV-19/Chile/RM-137638/2022
457 (XBB.1.5). Weight loss and survival were monitored for 6 days after challenge. At 3 and 6 days
458 post challenge, mouse lungs were collected for viral titration and histological analyses. All work
459 with live SARS-CoV-2 virus was performed in the Biosafety Level-3 (BSL-3) containment
460 laboratories.

461 **Enzyme-linked immunosorbent assay (ELISA)**

462 SARS-CoV-2 spike- and influenza HA-specific IgG antibody titers were determined by ELISA.
463 96-well plates (JET BIOFIL) were coated with recombinant spike proteins of Wuhan-hu-1
464 (ACROBiosystems, SPN-C52H4), BA.2.75.2 (ACROBiosystems, SPN-C522r), BQ.1.1
465 (ACROBiosystems, SPN-C522), or XBB.1.5 variant (ACROBiosystems, SPN-C524i), or
466 recombinant Influenza HA proteins of A/Wisconsin/588/2019/A/Victoria/2570/2019 (H1N1)
467 (Sinobiological, 40787-V08H1), A/Darwin/6/2021 (H3N2) (Sinobiological, 40868-V08H),
468 B/PHUKET/3073/2013 (Sinobiological, 40498-V08B), B/Austria/1359417/2021 (Sinobiological,
469 40862-V08H), A/Vietnam/1194/2004 (H5N1) (Sinobiological, 11062-V08H1), or
470 A/Hangzhou/3/2013 (H7N9) (Sinobiological, 40123-V08B) with a concentration of 2 µg/ml at
471 4°C overnight. The plates were washed three times with PBS containing 0.1% Tween 20 (PBST)
472 and subsequently blocked with 1% bovine serum albumin in PBST at 37°C for 1 h. After blocking,
473 100 µl of serial dilutions of heat-inactivated serum sample was added to the plates, followed by
474 incubation at 37°C for 1 h. Following thorough washes, HRP-conjugated Goat anti-mouse IgG
475 (H+L) antibody (Proteintech, SA00001-1) was added to the plates and incubated at 37°C for 1 h.
476 After three additional washes, 100 µL of TMB peroxidase substrate (TIANGEN, PA107-02) was
477 added to each well and incubated for 15 min before being stopped by adding 2 M H₂SO₄, and the
478 absorbance was measured at 450 nm using a TECAN Infinite M200 Pro plate reader. Endpoint
479 titers were determined as the reciprocal of the highest serum dilution that exceeded the cut-off
480 values (calculated as the mean ± SD of negative controls at the lowest dilution).

481 **Micro-neutralization (MN) assay**

482 To determine neutralizing antibody titers against influenza viruses, mouse serum samples were
483 treated with receptor-destroying enzyme II (RDE II) (Denka-Seiken) for 16 h at 37°C, followed by
484 heat-inactivation for 30 min at 56°C. The MN assays were performed as previously described (31).
485 To determine neutralizing antibody titers against SARS-CoV-2 viruses, serum samples collected
486 from immunized mice were inactivated at 56 °C for 30 min and the MN assays were performed as
487 described elsewhere (12). The MN titer was defined as the reciprocal of the highest serum dilution
488 capable of neutralizing 50% of viral infections in MDCK cells (for influenza viral titers) or Vero
489 E6 cells (for SARS-CoV-2 viral titers). The minimum MN titer detected in this study was 10; thus,
490 for statistical purposes, all samples from which the MN titer was not detected were given a
491 numeric value of 5, which represents the undetectable level of MN titer.

492 **ELISpot**

493 Cellular immune responses were determined by using IFN-γ (Dakewe Biotech, 2210005), IL-2
494 (Mabtech, 3441-4HPW-2), IL-4 (Dakewe Biotech, 2210402), and IL-5 (Mabtech, 3391-4HPW-2)

495 precoated ELISpot kits according to the manufacturer's instructions. Briefly, Spleen lymphocytes
496 isolated from BALB/c mice 14 days after the booster vaccination and plated at 2.5×10^5 cells/well
497 were added to the pre-coated plates. The spleen lymphocytes were stimulated with 1 μ g/ml
498 recombinant spike proteins or HA proteins and cultured at and 37°C and 5% CO₂ for 20 h.
499 Concanavalin A (Sigma) was used as a positive control, and RPMI 1640 medium (Gibco, Thermo
500 Fisher Scientific) was used as a negative control. The plates were then washed 6 times with wash
501 buffer and incubated for 1 h with biotinylated anti-mouse IFN- γ , IL-2, IL-4, or IL-5 antibody.
502 Streptavidin-HRP was added to the plates and incubated for 1 h. After the final washes, the AEC
503 substrate solution was added and stopped with water. The air-dried plates were read by using
504 ELISpotreader.

505 **Infectious viral titration by TCID₅₀.**

506 The right lung lobes were homogenized in 0.5 DMEM containing 0.3% BSA (Sigma-Aldrich)
507 and 1% penicillin/streptomycin (Gibco, Thermo Fisher Scientific) for 1 min at 6,000 rpm by using
508 a homogenizer (Servicebio). The turbinate was homogenized in 1 ml of the same medium. The
509 debris were pelleted by centrifugation for 10 min at 12,000 \times g. Their infectious virus titers were
510 determined by TCID₅₀ with MDCK cells (for influenza viral titers) or Vero E6 cells (for
511 SARS-CoV-2 viral titers) as previously described (64, 65).

512 **Histopathology.**

513 Mouse left lung lobes were fixed in 10% buffered formalin, paraffin-embedded, sectioned at 4
514 μ m, and stained with hematoxylin and eosin (H&E) for histopathological examination.

515

516 **Phylogenetic analysis**

517 The phylogenetic analysis was performed as described previously (46). All available full-length
518 HA genes collected during January 1, 2000, to June 30, 2023 for the influenza A(H1N1)
519 (2009-present), A/H3N2 (2000-present), A/H5, A/H7, B/Yamagata, B/Victoria viruses, and spike
520 genes for SARS-CoV-2 ancestral strains and omicron variants were downloaded from GISAID. To
521 contextualize the sequences of vaccine strains and challenge strains, we utilized the Nextstrain
522 pipeline (66) to build two separate phylogenetic trees: one for influenza HAs (A/H1, A/H3, A/H5,
523 A/H7, B/Yamagata, and B/Victoria) and the other for SARS-CoV-2 spikes (30). For influenza tree,
524 we randomly subsampled 10 sequences per HA type (for influenza A sequences) or lineage (for
525 influenza B sequences) for each year. We excluded duplicate sequences, any sequences sampled
526 before 2000, and sequences with incomplete collection dates or non-nucleotide characters. For the
527 SARS-CoV-2 tree, we randomly subsampled approximately 1000 sequences from the omicron
528 lineages based on the pre-analysis results from the Nextstrain pipeline. Following subsampling,
529 sequences were aligned using MAFFT (67), and divergence phylogenies were constructed with
530 IQ-TREE under a General Time Reversible (GTR) substitution model (68). Finally, tree plotting
531 and visualization were carried out using ggtree
532 (<https://guangchuangyu.github.io/software/ggtree/>).

533 **Statistical analyses.**

534 Statistical analyses were conducted using GraphPad Prism version 9. Data are presented as
535 geometric means \pm 95% CI for antibody titers, and means \pm SEM for all other data. For statistical
536 significance testing, an unpaired *t* test was applied when data showed equal variation between
537 groups, and Welch's *t* test was used for data with unequal variation. For comparisons involving
538 multiple groups, one-way ANOVA with Tukey's post-hoc test was employed. To achieve normality,

539 antibody titer data were log-transformed prior to analysis. A *P* value of less than 0.05 was
540 considered statistically significant.
541

542 **Acknowledgements**

543 The authors thank Yi Fang for her assistance in phylogenetic analyses and thank Qiuwen Tang
544 for his support in the animal studies. We sincerely thank Dr. George Dacai Liu for his comments
545 and assistance in revising our manuscript. This work was supported by National Key R&D
546 Program of China (2021YFC1712904), National Natural Science Foundation of China (82174053,
547 82361168672, 81761128014 and 31970884), Natural Science Foundation of Guangdong Province
548 (2022A1515010301), Macao Science and Technology Development Fund (0022/2021/A1 and
549 005/2022/ALC), Guangzhou Science and Technology Bureau project (202201020523,
550 202201020449), The Young Top Talent of Science and Technology Innovation Department of
551 Guangdong Province (2021TQ060189), The Youth Lift Project of China Association for Science
552 and Technology (2020-2022QNRC001), Open Project of State Key Laboratory of Respiratory
553 Disease (SKLRD-OP-202001 and SKLRD-OP-202209), Self-supporting Program of Guangzhou
554 Laboratory, Grant No. SRPG22-007, and Guangdong-Hong Kong-Macao Joint Laboratory of
555 Respiratory Infectious Diseases Funding Project (GHMJLRID-Z-202105).
556

557 **Competing interests**

558 The authors declared that they have no conflicts of interest to this work.
559

560 **References**

- 561 1. Organization WH. WHO Coronavirus (COVID-19) Dashboard 2023 [Available
562 from: <https://covid19.who.int/>.
- 563 2. Vasconcelos GL, Pessoa NL, Silva NB, Macedo AMS, Brum AA, Ospina R, et al.
564 Multiple waves of COVID-19: a pathway model approach. *Nonlinear Dyn.*
565 2023;111(7):6855-72.
- 566 3. Organization WH. Statement on the fifteenth meeting of the IHR (2005)
567 Emergency Committee on the COVID-19 pandemic 2023 [updated 5 May 2023].
568 Available from:
569 [https://www.who.int/news/item/05-05-2023-statement-on-the-fifteenth-meeting-of-the-](https://www.who.int/news/item/05-05-2023-statement-on-the-fifteenth-meeting-of-the-international-health-regulations-(2005)-emergency-committee-regarding-the-coronavirus-disease-(covid-19)-pandemic)
570 [international-health-regulations-\(2005\)-emergency-committee-regarding-the-coronav-](https://www.who.int/news/item/05-05-2023-statement-on-the-fifteenth-meeting-of-the-international-health-regulations-(2005)-emergency-committee-regarding-the-coronavirus-disease-(covid-19)-pandemic)
571 [irus-disease-\(covid-19\)-pandemic](https://www.who.int/news/item/05-05-2023-statement-on-the-fifteenth-meeting-of-the-international-health-regulations-(2005)-emergency-committee-regarding-the-coronavirus-disease-(covid-19)-pandemic).
- 572 4. Krammer F, Ellebedy AH. Variant-adapted COVID-19 booster vaccines. *Science.*
573 2023;382(6667):157-9.
- 574 5. Organization WH. Influenza (Seasonal) 2023 [updated 3 October, 2023. Available
575 from: [https://www.who.int/news-room/fact-sheets/detail/influenza-\(seasonal\)](https://www.who.int/news-room/fact-sheets/detail/influenza-(seasonal)).
- 576 6. Wang Y, Tang CY, Wan XF. Antigenic characterization of influenza and
577 SARS-CoV-2 viruses. *Anal Bioanal Chem.* 2022;414(9):2841-81.
- 578 7. Furlow B. Triple-demic overwhelms paediatric units in US hospitals. *Lancet*
579 *Child Adolesc Health.* 2023;7(2):86.

- 580 8. Koutsakos M, Kedzierska K, Subbarao K. Immune Responses to Avian Influenza
581 Viruses. *Journal of immunology*. 2019;202(2):382-91.
- 582 9. Organization WH. Ongoing avian influenza outbreaks in animals pose risk to
583 humans 2023 [updated 12 July 2023. Available from:
584 [https://www.who.int/news/item/12-07-2023-ongoing-avian-influenza-outbreaks-in-ani](https://www.who.int/news/item/12-07-2023-ongoing-avian-influenza-outbreaks-in-animals-pose-risk-to-humans)
585 [mals-pose-risk-to-humans](https://www.who.int/news/item/12-07-2023-ongoing-avian-influenza-outbreaks-in-animals-pose-risk-to-humans).
- 586 10. Organization WH. Avian Influenza Weekly Update Number 920 2023 [updated 3
587 November, 2023. Available from:
588 https://cdn.who.int/media/docs/default-source/wpro---documents/emergency/surveillance/avian-influenza/ai_20231103.pdf?sfvrsn=5bc7c406_33.
589
- 590 11. Ma Q, Li R, Guo J, Li M, Ma L, Dai J, et al. Immunization with a Prefusion
591 SARS-CoV-2 Spike Protein Vaccine (RBMRNA-176) Protects against Viral
592 Challenge in Mice and Nonhuman Primates. *Vaccines*. 2022;10(10).
- 593 12. Ma Q, Li M, Ma L, Zhang C, Zhang H, Zhong H, et al. SARS-CoV-2 bivalent
594 mRNA vaccine with broad protection against variants of concern. *Front Immunol*.
595 2023;14:1195299.
- 596 13. Polack FP, Thomas SJ, Kitchin N, Absalon J, Gurtman A, Lockhart S, et al.
597 Safety and Efficacy of the BNT162b2 mRNA Covid-19 Vaccine. *The New England*
598 *journal of medicine*. 2020;383(27):2603-15.
- 599 14. Baden LR, El Sahly HM, Essink B, Kotloff K, Frey S, Novak R, et al. Efficacy
600 and Safety of the mRNA-1273 SARS-CoV-2 Vaccine. *The New England journal of*
601 *medicine*. 2021;384(5):403-16.
- 602 15. Creech CB, Walker SC, Samuels RJ. SARS-CoV-2 Vaccines. *Jama*.
603 2021;325(13):1318-20.
- 604 16. Karim SSA, Karim QA. Omicron SARS-CoV-2 variant: a new chapter in the
605 COVID-19 pandemic. *Lancet*. 2021;398(10317):2126-8.
- 606 17. Zhao Z, Zhou J, Tian M, Huang M, Liu S, Xie Y, et al. Omicron SARS-CoV-2
607 mutations stabilize spike up-RBD conformation and lead to a non-RBM-binding
608 monoclonal antibody escape. *Nature communications*. 2022;13(1):4958.
- 609 18. Chalkias S, Feng J, Chen X, Zhou H, Marshall JC, Girard B, et al. Neutralization
610 of Omicron Subvariant BA.2.75 after Bivalent Vaccination. *The New England journal*
611 *of medicine*. 2022;387(23):2194-6.
- 612 19. Chalkias S, Harper C, Vrbicky K, Walsh SR, Essink B, Brosz A, et al. A Bivalent
613 Omicron-Containing Booster Vaccine against Covid-19. *The New England journal of*
614 *medicine*. 2022;387(14):1279-91.
- 615 20. Davis-Gardner ME, Lai L, Wali B, Samaha H, Solis D, Lee M, et al.
616 Neutralization against BA.2.75.2, BQ.1.1, and XBB from mRNA Bivalent Booster. *N*
617 *Engl J Med*. 2023;388(2):183-5.
- 618 21. Zou J, Kurhade C, Patel S, Kitchin N, Tompkins K, Cutler M, et al. Improved
619 Neutralization of Omicron BA.4/5, BA.4.6, BA.2.75.2, BQ.1.1, and XBB.1 with
620 Bivalent BA.4/5 Vaccine. *bioRxiv*. 2022:2022.11.17.516898.
- 621 22. Davis-Gardner ME, Lai L, Wali B, Samaha H, Solis D, Lee M, et al.
622 Neutralization against BA.2.75.2, BQ.1.1, and XBB from mRNA Bivalent Booster.
623 *The New England journal of medicine*. 2022.

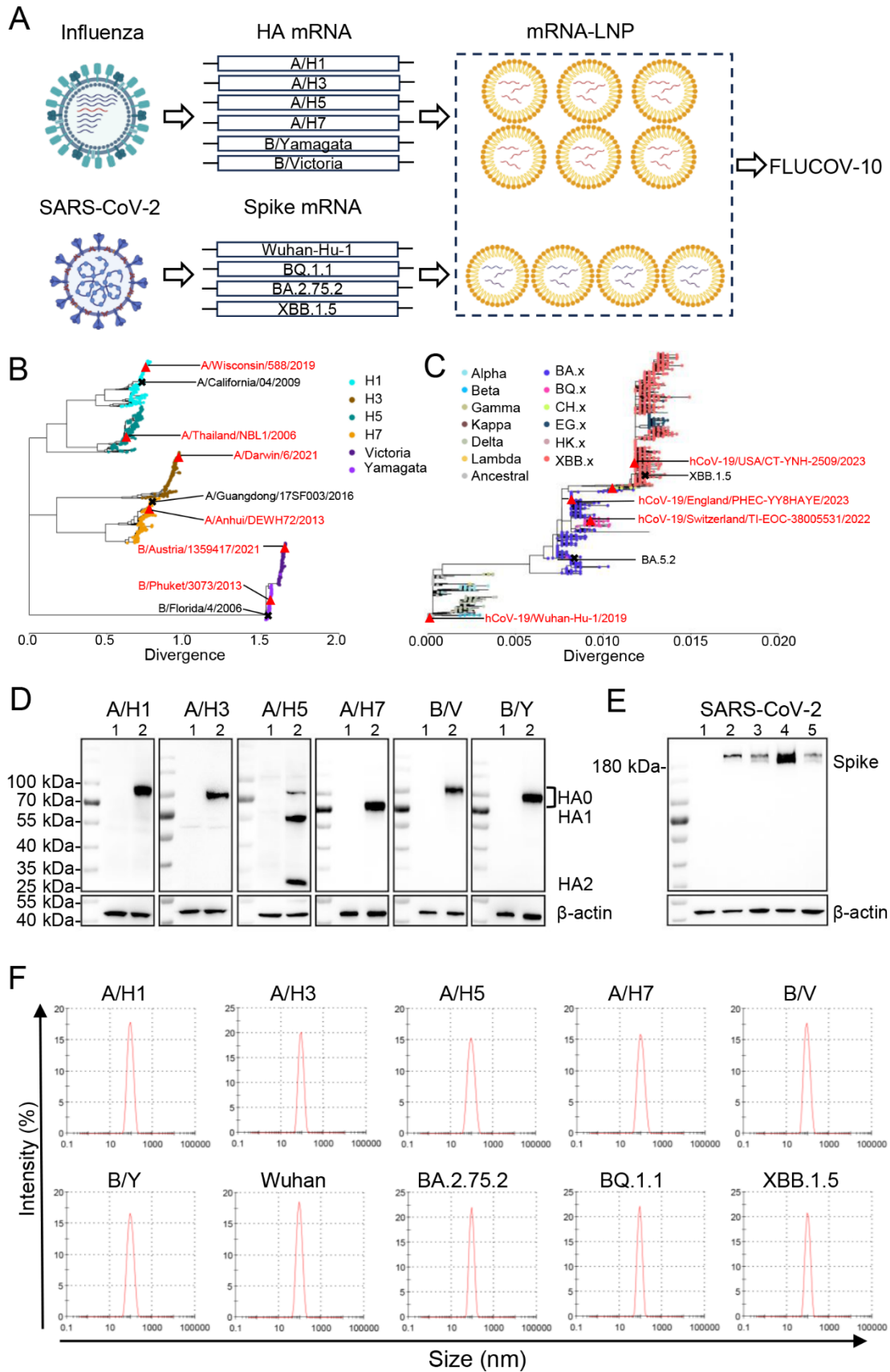
- 624 23. Feldman RA, Fuhr R, Smolenov I, Mick Ribeiro A, Panther L, Watson M, et al.
625 mRNA vaccines against H10N8 and H7N9 influenza viruses of pandemic potential
626 are immunogenic and well tolerated in healthy adults in phase 1 randomized clinical
627 trials. *Vaccine*. 2019;37(25):3326-34.
- 628 24. Lee IT, Nachbagauer R, Ensz D, Schwartz H, Carmona L, Schaeffers K, et al.
629 Safety and immunogenicity of a phase 1/2 randomized clinical trial of a quadrivalent,
630 mRNA-based seasonal influenza vaccine (mRNA-1010) in healthy adults: interim
631 analysis. *Nature communications*. 2023;14(1):3631.
- 632 25. moderna. Moderna Announces Interim Phase 3 Safety and Immunogenicity
633 Results for mRNA-1010, a Seasonal Influenza Vaccine Candidate 2023 [updated 16
634 February, 2023. Available from:
635 [https://www.accesswire.com/739660/Moderna-Announces-Interim-Phase-3-Safety-an](https://www.accesswire.com/739660/Moderna-Announces-Interim-Phase-3-Safety-and-Immunogenicity-Results-for-mRNA-1010-a-Seasonal-Influenza-Vaccine-Candidate)
636 [d-Immunogenicity-Results-for-mRNA-1010-a-Seasonal-Influenza-Vaccine-Candidate](https://www.accesswire.com/739660/Moderna-Announces-Interim-Phase-3-Safety-and-Immunogenicity-Results-for-mRNA-1010-a-Seasonal-Influenza-Vaccine-Candidate)
637 .
- 638 26. Organization WH. Antigenic and genetic characteristics of zoonotic influenza A
639 viruses and development of candidate vaccine viruses for pandemic preparedness
640 2022 [updated September 2022. Available from:
641 [https://cdn.who.int/media/docs/default-source/influenza/who-influenza-recommendati](https://cdn.who.int/media/docs/default-source/influenza/who-influenza-recommendations/vcm-southern-hemisphere-recommendation-2023/202209_zoonotic_vaccinivirusupdate.pdf)
642 [ons/vcm-southern-hemisphere-recommendation-2023/202209_zoonotic_vaccinivirusu](https://cdn.who.int/media/docs/default-source/influenza/who-influenza-recommendations/vcm-southern-hemisphere-recommendation-2023/202209_zoonotic_vaccinivirusupdate.pdf)
643 [pdate.pdf](https://cdn.who.int/media/docs/default-source/influenza/who-influenza-recommendations/vcm-southern-hemisphere-recommendation-2023/202209_zoonotic_vaccinivirusupdate.pdf).
- 644 27. Data OWi. SARS-CoV-2 sequences by variant, Nov 20, 2023 2023 [updated
645 November 20, 2023. Available from:
646 <https://ourworldindata.org/grapher/covid-variants-bar>.
- 647 28. Kurhade C, Zou J, Xia H, Liu M, Chang HC, Ren P, et al. Low neutralization of
648 SARS-CoV-2 Omicron BA.2.75.2, BQ.1.1 and XBB.1 by parental mRNA vaccine or
649 a BA.5 bivalent booster. *Nature medicine*. 2023;29(2):344-7.
- 650 29. Horimoto T, Nakayama K, Smeekens SP, Kawaoka Y. Proprotein-processing
651 endoproteases PC6 and furin both activate hemagglutinin of virulent avian influenza
652 viruses. *Journal of virology*. 1994;68(9):6074-8.
- 653 30. Stieneke-Grober A, Vey M, Angliker H, Shaw E, Thomas G, Roberts C, et al.
654 Influenza virus hemagglutinin with multibasic cleavage site is activated by furin, a
655 subtilisin-like endoprotease. *EMBO J*. 1992;11(7):2407-14.
- 656 31. Wang Y, Lv Y, Niu X, Dong J, Feng P, Li Q, et al. L226Q Mutation on Influenza
657 H7N9 Virus Hemagglutinin Increases Receptor-Binding Avidity and Leads to Biased
658 Antigenicity Evaluation. *Journal of virology*. 2020;94(20).
- 659 32. Dong J, Chen P, Wang Y, Lv Y, Xiao J, Li Q, et al. Evaluation of the immune
660 response of a H7N9 candidate vaccine virus derived from the fifth wave
661 A/Guangdong/17SF003/2016. *Antiviral research*. 2020:104776.
- 662 33. Bao L, Deng W, Qi F, Lv Q, Song Z, Liu J, et al. Sequential infection with H1N1
663 and SARS-CoV-2 aggravated COVID-19 pathogenesis in a mammalian model, and
664 co-vaccination as an effective method of prevention of COVID-19 and influenza.
665 *Signal Transduct Target Ther*. 2021;6(1):200.
- 666 34. Shi R, Zeng J, Xu L, Wang F, Duan X, Wang Y, et al. A combination vaccine
667 against SARS-CoV-2 and H1N1 influenza based on receptor binding domain

- 668 trimerized by six-helix bundle fusion core. *EBioMedicine*. 2022;85:104297.
- 669 35. Massare MJ, Patel N, Zhou B, Maciejewski S, Flores R, Guebre-Xabier M, et al.
670 Combination Respiratory Vaccine Containing Recombinant SARS-CoV-2 Spike and
671 Quadrivalent Seasonal Influenza Hemagglutinin Nanoparticles with Matrix-M
672 Adjuvant. 2021:2021.05.05.442782.
- 673 36. Ye Q, Wu M, Zhou C, Lu X, Huang B, Zhang N, et al. Rational development of a
674 combined mRNA vaccine against COVID-19 and influenza. *NPJ vaccines*.
675 2022;7(1):84.
- 676 37. Pfizer. Pfizer and BioNTech Announce Positive Topline Data for mRNA-based
677 Combination Vaccine Program Against Influenza and COVID-19 2023 [updated
678 October 26, 2023. Available from:
679 [https://www.pfizer.com/news/press-release/press-release-detail/pfizer-and-biontech-an-](https://www.pfizer.com/news/press-release/press-release-detail/pfizer-and-biontech-announce-positive-topline-data-mrna)
680 [nounce-positive-topline-data-mrna](https://www.pfizer.com/news/press-release/press-release-detail/pfizer-and-biontech-announce-positive-topline-data-mrna).
- 681 38. Moderna. Moderna Announces Positive Phase 1/2 Data from mRNA-1083, the
682 Company's Combination Vaccine Against Influenza and COVID-19 2023 [updated
683 October 4, 2023. Available from:
684 [https://investors.modernatx.com/news/news-details/2023/Moderna-Announces-Positiv-](https://investors.modernatx.com/news/news-details/2023/Moderna-Announces-Positive-Phase-1-2-Data-from-mRNA-1083-the-Company-s-Combination-Vaccine-Against-Influenza-and-COVID-19/default.aspx)
685 [e-Phase-1-2-Data-from-mRNA-1083-the-Company-s-Combination-Vaccine-Against-In-](https://investors.modernatx.com/news/news-details/2023/Moderna-Announces-Positive-Phase-1-2-Data-from-mRNA-1083-the-Company-s-Combination-Vaccine-Against-Influenza-and-COVID-19/default.aspx)
686 [fluenza-and-COVID-19/default.aspx](https://investors.modernatx.com/news/news-details/2023/Moderna-Announces-Positive-Phase-1-2-Data-from-mRNA-1083-the-Company-s-Combination-Vaccine-Against-Influenza-and-COVID-19/default.aspx).
- 687 39. Tafreshi SH. Efficacy, safety, and formulation issues of the combined vaccines.
688 *Expert Rev Vaccines*. 2020;19(10):949-58.
- 689 40. Tsang TK, Cauchemez S, Perera RA, Freeman G, Fang VJ, Ip DK, et al.
690 Association between antibody titers and protection against influenza virus infection
691 within households. 2014;210(5):684-92.
- 692 41. Khoury DS, Cromer D, Reynaldi A, Schlub TE, Wheatley AK, Juno JA, et al.
693 Neutralizing antibody levels are highly predictive of immune protection from
694 symptomatic SARS-CoV-2 infection. 2021;27(7):1205-11.
- 695 42. Pardi N, Parkhouse K, Kirkpatrick E, McMahon M, Zost SJ, Mui BL, et al.
696 Nucleoside-modified mRNA immunization elicits influenza virus hemagglutinin
697 stalk-specific antibodies. *Nature communications*. 2018;9(1):3361.
- 698 43. Impagliazzo A, Milder F, Kuipers H, Wagner MV, Zhu X, Hoffman RM, et al. A
699 stable trimeric influenza hemagglutinin stem as a broadly protective immunogen.
700 *Science*. 2015;349(6254):1301-6.
- 701 44. Cowling BJ, Perera R, Valkenburg SA, Leung NHL, Iuliano AD, Tam YH, et al.
702 Comparative Immunogenicity of Several Enhanced Influenza Vaccine Options for
703 Older Adults: A Randomized, Controlled Trial. *Clinical infectious diseases : an*
704 *official publication of the Infectious Diseases Society of America*.
705 2020;71(7):1704-14.
- 706 45. Reneer ZB, Bergeron HC, Reynolds S, Thornhill-Wadolowski E, Feng L, Bugno
707 M, et al. mRNA Vaccines Encoding Influenza Virus Hemagglutinin (HA) Elicits
708 Immunity in Mice from Influenza A Virus Challenge. 2023:2023.11.15.566914.
- 709 46. Arevalo CP, Bolton MJ, Le Sage V, Ye N, Furey C, Muramatsu H, et al. A
710 multivalent nucleoside-modified mRNA vaccine against all known influenza virus
711 subtypes. *Science*. 2022;378(6622):899-904.

- 712 47. Scheaffer SM, Lee D, Whitener B, Ying B, Wu K, Liang CY, et al. Bivalent
713 SARS-CoV-2 mRNA vaccines increase breadth of neutralization and protect against
714 the BA.5 Omicron variant in mice. *Nature medicine*. 2023;29(1):247-57.
- 715 48. Zeng J, Li Y, Jiang L, Luo L, Wang Y, Wang H, et al. Mpox multi-antigen mRNA
716 vaccine candidates by a simplified manufacturing strategy afford efficient protection
717 against lethal orthopoxvirus challenge. *Emerging microbes & infections*.
718 2023;12(1):2204151.
- 719 49. Menegale F, Manica M, Zardini A, Guzzetta G, Marziano V, d'Andrea V, et al.
720 Evaluation of Waning of SARS-CoV-2 Vaccine-Induced Immunity: A Systematic
721 Review and Meta-analysis. *JAMA Netw Open*. 2023;6(5):e2310650.
- 722 50. Markov PV, Ghafari M, Beer M, Lythgoe K, Simmonds P, Stilianakis NI, et al.
723 The evolution of SARS-CoV-2. *Nature reviews Microbiology*. 2023;21(6):361-79.
- 724 51. Doyon-Plourde P, Przepiorkowski J, Young K, Zhao L, Sinilaite A. Intraseasonal
725 waning immunity of seasonal influenza vaccine - A systematic review and
726 meta-analysis. *Vaccine*. 2023;41(31):4462-71.
- 727 52. Petrova VN, Russell CA. The evolution of seasonal influenza viruses. *Nature*
728 *Reviews Microbiology*. 2018;16(1):47-+.
- 729 53. Wiemken TL, Khan F, Puzniak L, Yang W, Simmering J, Polgreen P, et al.
730 Seasonal trends in COVID-19 cases, hospitalizations, and mortality in the United
731 States and Europe. *Scientific reports*. 2023;13(1):3886.
- 732 54. Skibinski DA, Baudner BC, Singh M, O'Hagan DT. Combination vaccines. *J*
733 *Glob Infect Dis*. 2011;3(1):63-72.
- 734 55. Tzenios N, Tazanios ME, Chahine M. Combining Influenza and COVID-19
735 Booster Vaccination Strategy to Improve Vaccination Uptake Necessary for Managing
736 the Health Pandemic: A Systematic Review and Meta-Analysis. *Vaccines*. 2022;11(1).
- 737 56. Belongia EA, Skowronski DM, McLean HQ, Chambers C, Sundaram ME, De
738 Serres G. Repeated annual influenza vaccination and vaccine effectiveness: review of
739 evidence. *Expert Rev Vaccines*. 2017;16(7):1-14.
- 740 57. Thompson MG, Cowling BJ. How repeated influenza vaccination effects might
741 apply to COVID-19 vaccines. *Lancet Respir Med*. 2022;10(7):636-8.
- 742 58. Pan W, Dong Z, Meng W, Zhang W, Li T, Li C, et al. Improvement of influenza
743 vaccine strain A/Vietnam/1194/2004 (H5N1) growth with the neuraminidase
744 packaging sequence from A/Puerto Rico/8/34. *Human vaccines &*
745 *immunotherapeutics*. 2012;8(2):252-9.
- 746 59. Thran M, Mukherjee J, Ponisch M, Fiedler K, Thess A, Mui BL, et al. mRNA
747 mediates passive vaccination against infectious agents, toxins, and tumors. *EMBO*
748 *Mol Med*. 2017;9(10):1434-47.
- 749 60. Thess A, Grund S, Mui BL, Hope MJ, Baumhof P, Fotin-Mleczek M, et al.
750 Sequence-engineered mRNA Without Chemical Nucleoside Modifications Enables an
751 Effective Protein Therapy in Large Animals. *Molecular therapy : the journal of the*
752 *American Society of Gene Therapy*. 2015;23(9):1456-64.
- 753 61. Holtkamp S, Kreiter S, Selmi A, Simon P, Koslowski M, Huber C, et al.
754 Modification of antigen-encoding RNA increases stability, translational efficacy, and
755 T-cell stimulatory capacity of dendritic cells. *Blood*. 2006;108(13):4009-17.

- 756 62. Kariko K, Muramatsu H, Ludwig J, Weissman D. Generating the optimal mRNA
757 for therapy: HPLC purification eliminates immune activation and improves
758 translation of nucleoside-modified, protein-encoding mRNA. *Nucleic acids research*.
759 2011;39(21):e142.
- 760 63. Patel S, Ryals RC, Weller KK, Pennesi ME, Sahay G. Lipid nanoparticles for
761 delivery of messenger RNA to the back of the eye. *J Control Release*.
762 2019;303:91-100.
- 763 64. Organization WH. Manual for the laboratory diagnosis and virological
764 surveillance of influenza 2011 [Available from:
765 [https://apps.who.int/iris/bitstream/handle/10665/44518/9789241548090_eng.pdf;jsess](https://apps.who.int/iris/bitstream/handle/10665/44518/9789241548090_eng.pdf;jsessionid=AF0FFCECE2F1C0F120B2A8C0B281272F?sequence=1)
766 [ionid=AF0FFCECE2F1C0F120B2A8C0B281272F?sequence=1](https://apps.who.int/iris/bitstream/handle/10665/44518/9789241548090_eng.pdf;jsessionid=AF0FFCECE2F1C0F120B2A8C0B281272F?sequence=1)].
- 767 65. Wang Y, Lench J, Kohler D, DeLiberto TJ, Tang CY, Li T, et al. SARS-CoV-2
768 Exposure in Norway Rats (*Rattus norvegicus*) from New York City. *mBio*.
769 2023;14(2):e0362122.
- 770 66. Hadfield J, Megill C, Bell SM, Huddleston J, Potter B, Callender C, et al.
771 Nextstrain: real-time tracking of pathogen evolution. *Bioinformatics*.
772 2018;34(23):4121-3.
- 773 67. Katoh K, Misawa K, Kuma K, Miyata T. MAFFT: a novel method for rapid
774 multiple sequence alignment based on fast Fourier transform. *Nucleic acids research*.
775 2002;30(14):3059-66.
- 776 68. Minh BQ, Schmidt HA, Chernomor O, Schrempf D, Woodhams MD, von
777 Haeseler A, et al. IQ-TREE 2: New Models and Efficient Methods for Phylogenetic
778 Inference in the Genomic Era. *Molecular biology and evolution*. 2020;37(5):1530-4.
779

780 **Figures and figure legends**

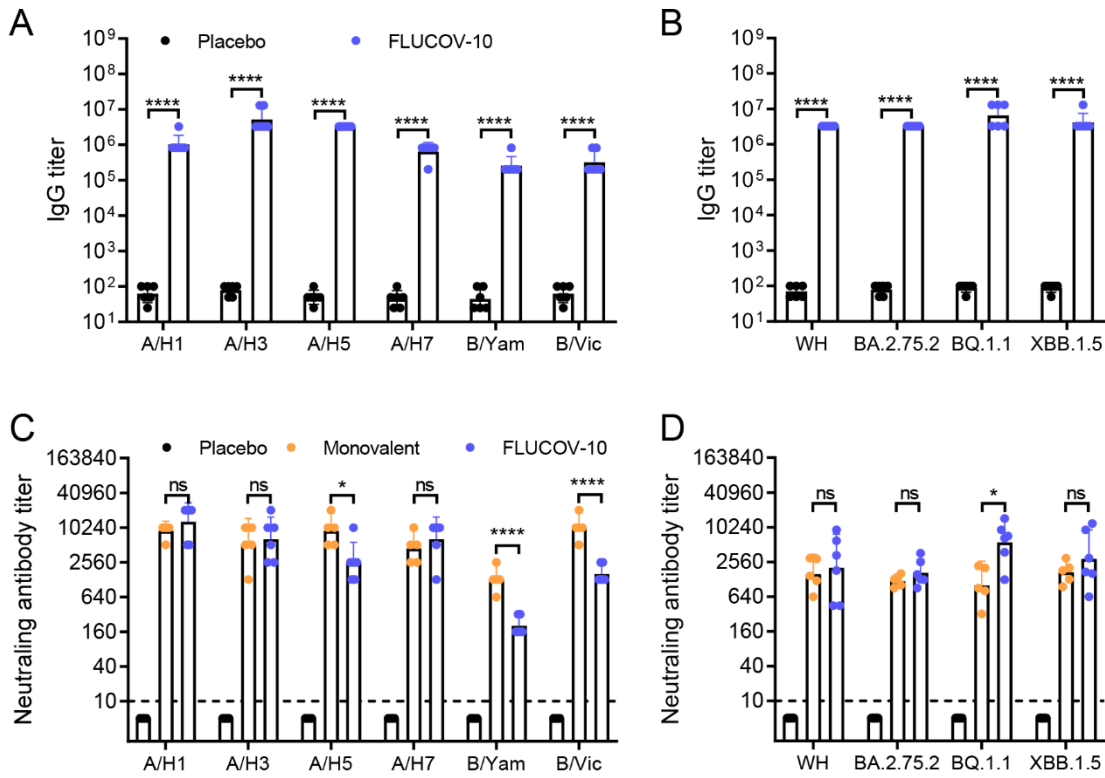


781

782 **Figure 1. Design and characterization of 10-valent mRNA vaccine (FLUCOV-10).**

783 A. Schematic illustration of the FLUCOV-10 formulation, a 10-valent combination mRNA
784 vaccine targeting both influenza and COVID-19. It includes mRNAs encoding the full-length HA
785 proteins from influenza A virus subtypes A/H1, A/H3, A/H5, and A/H7, and from influenza B
786 virus lineages B/Yamagata and B/Victoria. Additionally, it encodes full-length spike proteins from
787 SARS-CoV-2 variants Wuhan-Hu-1, BQ.1.1, BA.2.75.2, and XBB.1.5. Each mRNA component is
788 individually encapsulated in lipid nanoparticles (LNPs) prior to being combined into the final
789 FLUCOV-10 formulation. B and C. Phylogenetic trees were created for influenza HAs (B) and
790 SARS-CoV-2 spikes (C) by using Nextstrain. The vaccine HAs or spike are indicated with red
791 triangles and the challenge viruses are indicated with an “X”. D. Expression of
792 FLUCOV-10-mRNA-encoded HA proteins in 293T cells was determined by western blotting.
793 Lane 1, 293T cells with mock transfection; lane 2, 293T cells with indicated mRNA transfection;
794 E. Expression of FLUCOV-10-mRNA-encoded Spike proteins. Lane 1, 293T cells with mock
795 transfection; lane 2-5, 293T cells with Wuhan-Hu-1, BQ.1.1, BA.2.75.2, and XBB.1.5 mRNA
796 transfection, respectively. β -actin was used as western blotting loading control.

797



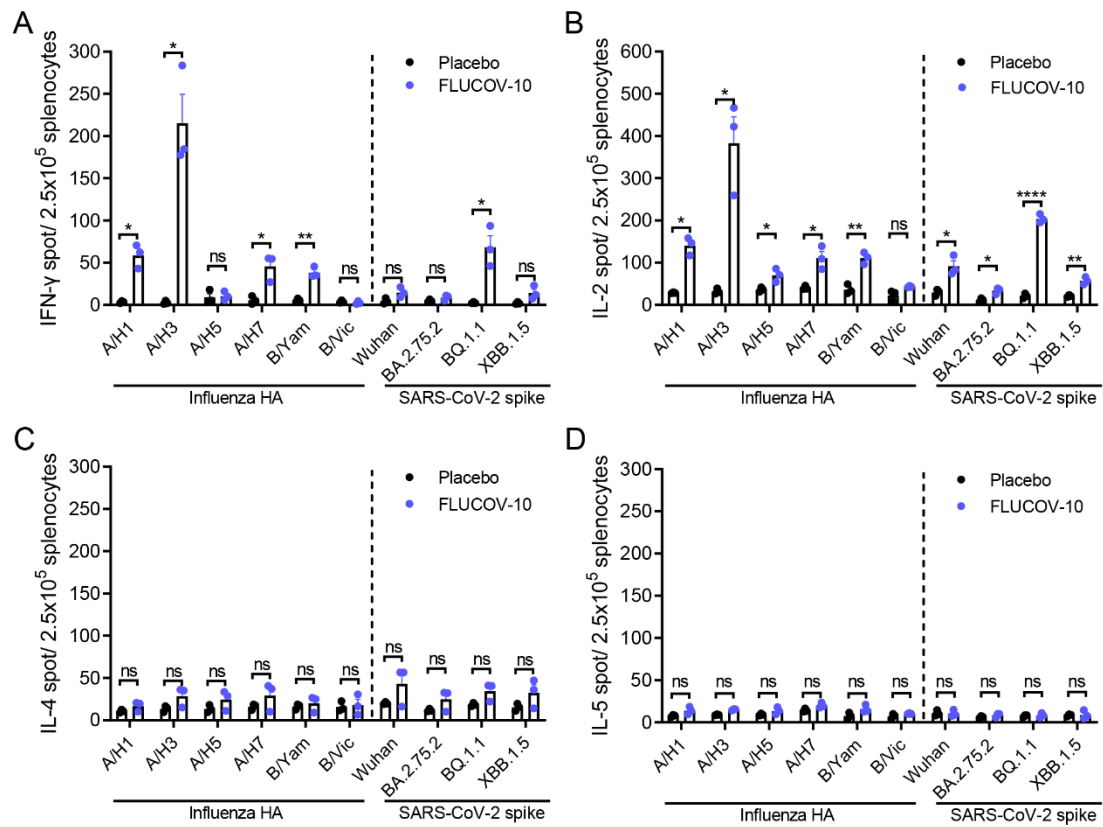
798

799

800 **Figure 2. FLUCOV-10 immunization elicits a robust humoral immune response in BALB/c**
 801 **mice.**

802 A and B. BALB/c mice were vaccinated intramuscularly (i.m.) with the FLUCOV-10 (a combined
 803 total dose of 50 μ g of mRNA, including 2.5 μ g of each mRNA) or a placebo. Vaccine matched
 804 influenza HA-specific (A) or SARS-CoV-2 spike-specific (B) IgG antibody titers 14 days post the
 805 second immunization were determined by ELISA. C and D. BALB/c mice were vaccinated i.m.
 806 with FLUCOV-10, monovalent mRNA vaccines (5 μ g) derived from each component of
 807 FLUCOV-10, or a placebo. Neutralizing antibody titers against vaccine matched influenza viruses
 808 (C) or SARS-CoV-2 viruses (D) were determined 14 days post second immunization by
 809 micro-neutralization assays. Data are presented as geometric means \pm 95% CI (n = 5 or 6). ns,
 810 non-significant; *, $p < 0.05$; **, $p < 0.001$; ***, $p < 0.0001$.

811



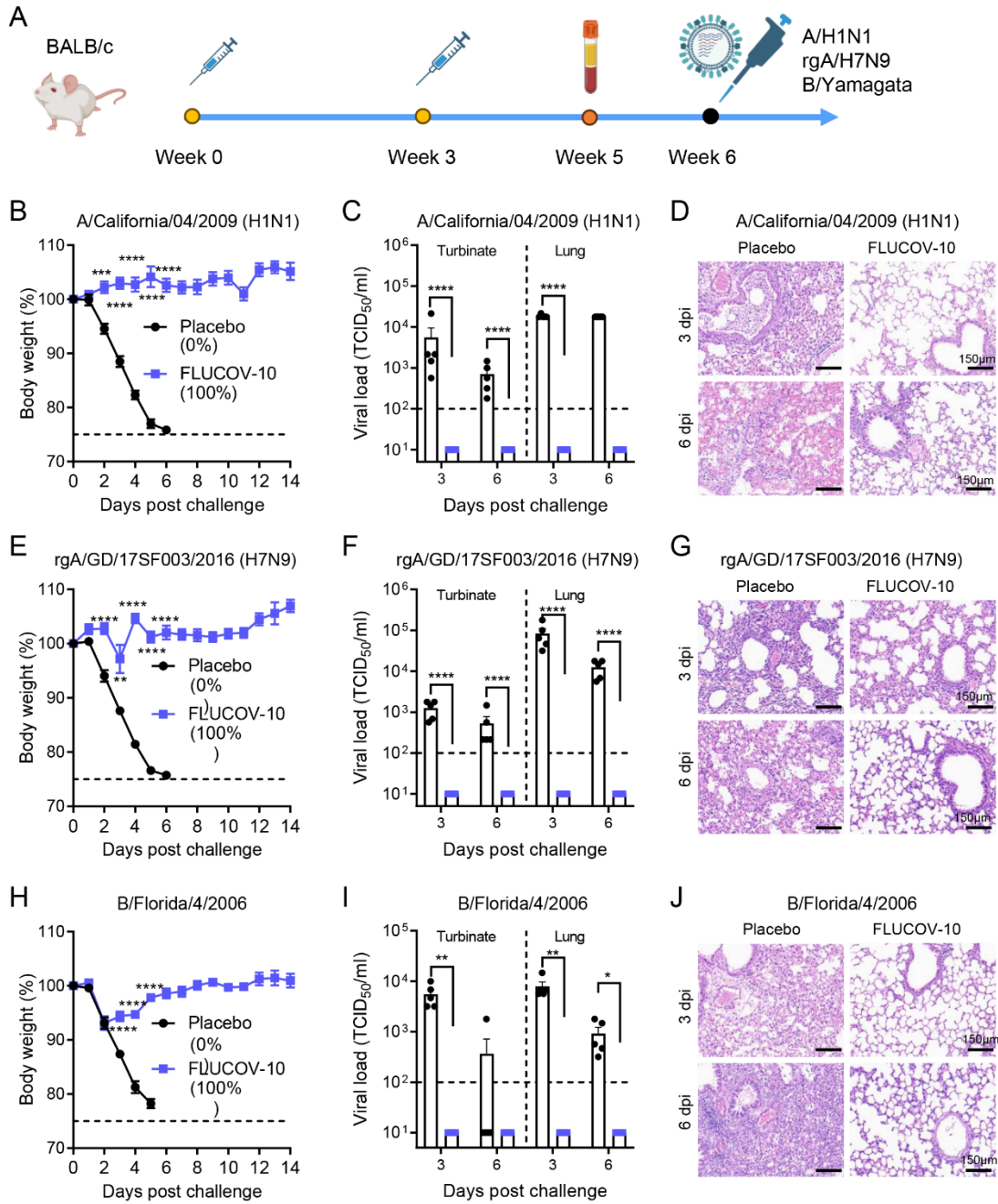
812

813

814 **Figure 3. FLUCOV-10 immunization elicits an antigen-specific Th1-biased cellular immune**
 815 **response in BALB/c mice.**

816 BALB/c mice were vaccinated intramuscularly (i.m.) with two doses of the FLUCOV-10 or a
 817 placebo, three weeks apart. Vaccine matched HA- or spike-specific splenocytes producing IFN- γ
 818 (A), IL-2 (B), IL-4 (C), or IL-5 (D) were determined 14 days post second immunization by
 819 ELISpot. Data are presented as mean \pm SEM (n = 3). ns, non-significant; *, $p < 0.05$; **, $p < 0.01$;
 820 ****, $p < 0.0001$.

821

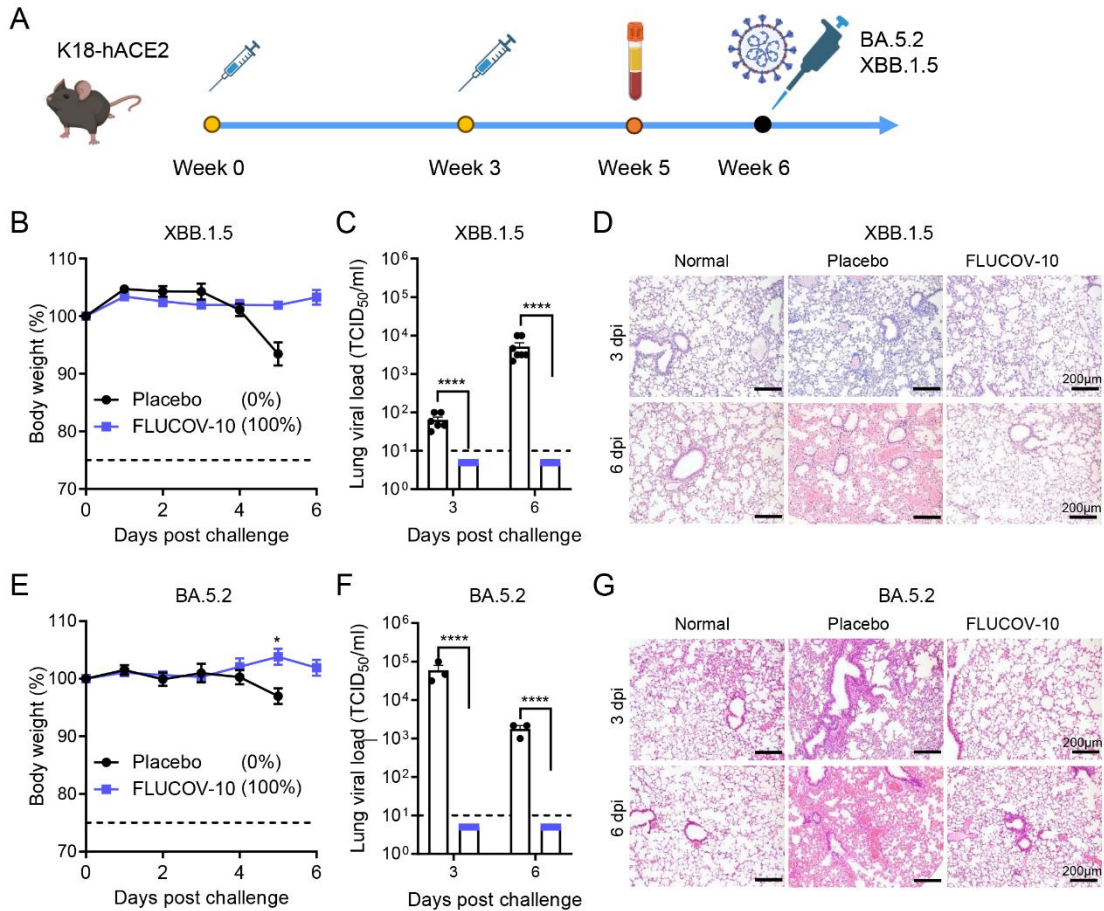


822

823 **Figure 4. FLUCOV-10 protects mice from homologous or heterologous challenge with**
 824 **influenza viruses.**

825 A. Schematic diagram of the experimental design. BALB/c Mice were immunized with 50 μ g of
 826 FLUCOV-10 or each volume of a placebo and boosted with the same dose after three weeks.
 827 Serum samples were collected 14 days post the second immunization. The mice were challenged 3
 828 weeks post second immunization with $10 \times$ mLD₅₀ of A/California/04/2009 (H1N1) (B-D) or $10 \times$
 829 mLD₅₀ of rgA/Guangdong/17SF003/2016 (H7N9) (E-G) or $3 \times$ mLD₅₀ of B/Florida/4/2006
 830 (B/Yamagata) (H-J). B, E, and H, Weight changes and survival rates were recorded for 14 days (n
 831 = 7). B, E, and H, Viral titers in the turbinate or lung tissues from influenza-infected mice (n = 5 at
 832 each indicated day). C, F, and I, H&E staining of lung tissues from influenza-infected mice.

833



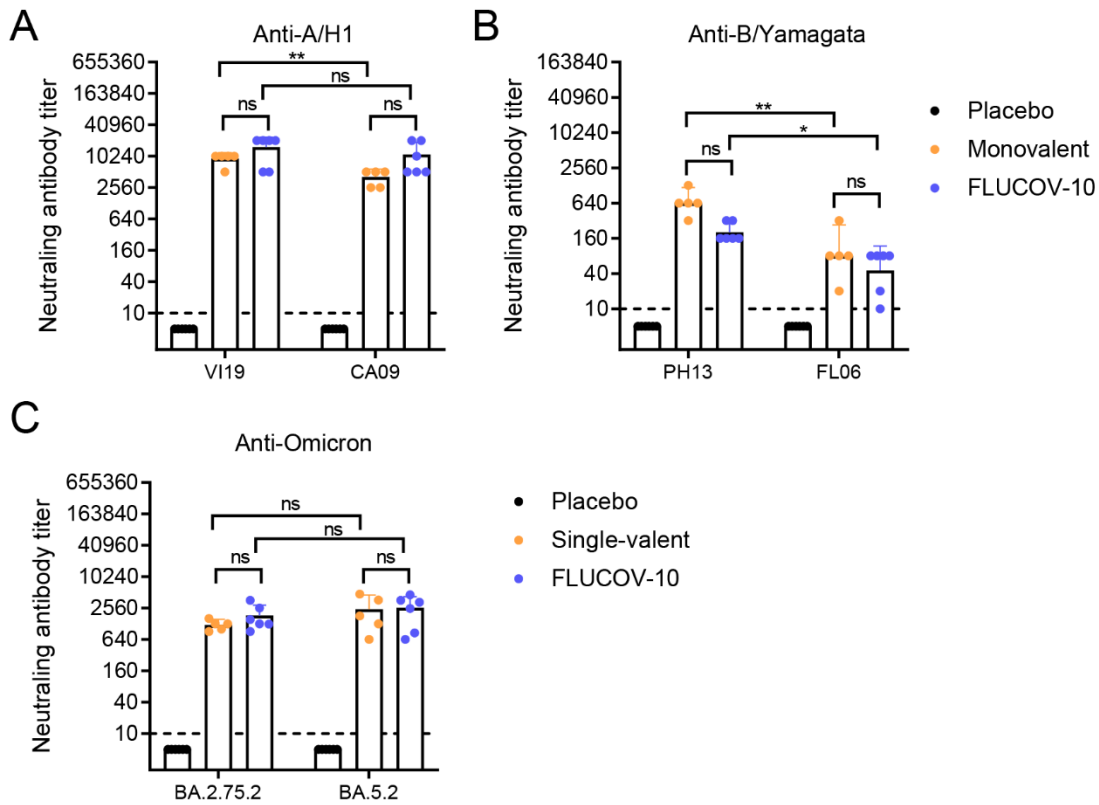
834

835 **Figure 5. FLUCOV-10 protects mice from challenge with SARS-CoV-2 viruses.**

836 A. Schematic diagram of the experimental design. K18-hACE2 mice were immunized with 50 μ g
 837 of FLUCOV-10 or each volume of a placebo and boosted with the same dose after three weeks.
 838 Serum samples were collected 14 days post the second immunization. The mice were challenged 3
 839 weeks post the second immunization with $10^{4.5}$ TCID₅₀ of hCoV-19/Chile/RM-137638/2022
 840 (XBB.1.5) (B-D) or 10^4 TCID₅₀ of hCoV-19/Uganda/UG1282/2022 (BA.5.2) (E-G). B and E,
 841 Weight changes and survival rates were recorded for 14 days (n = 7 or 4). C and F: Viral titers in
 842 the lung tissues from SARS-CoV-2-infected mice (n = 5 or 3 at each indicated day). D and G,
 843 H&E staining of lung tissues from infected or normal mice.

844

845 **Supplementary Information**

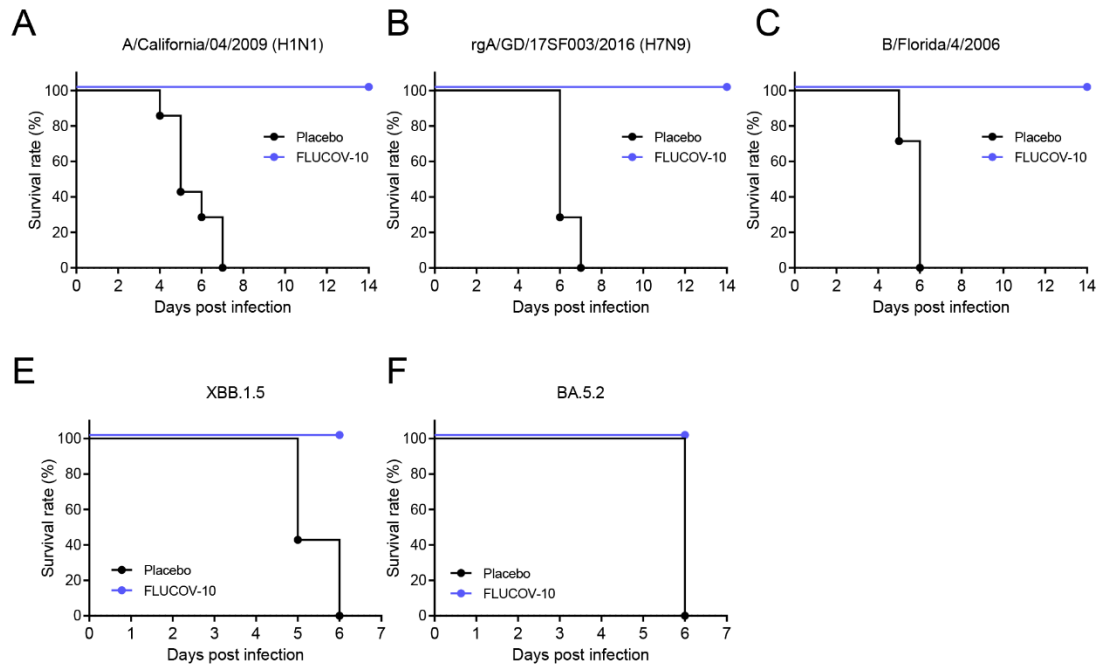


846

847 **Supplemental Figure 1. FLUCOV-10 immunization elicits a cross-reactive humoral immune**
 848 **response in BALB/c mice (related to Figure 2).**

849 A. BALB/c mice were vaccinated i.m. with the FLUCOV-10, monovalent A/H1 mRNA vaccines
 850 derived from FLUCOV-10 or a placebo. Neutralizing antibody titers against vaccine matched
 851 (A/Victoria/2570/2019, VI19) and antigenically distinct (A/California/04/2009, CA09)
 852 A/H1N1pdm09 influenza viruses were determined 14 days post second immunization by
 853 micro-neutralization assays. B. BALB/c mice were vaccinated i.m. with the FLUCOV-10,
 854 monovalent B/Yamagata mRNA vaccines derived from FLUCOV-10 or a placebo. Neutralizing
 855 antibody titers against vaccine matched (B/Phuket/3073/2013, PH13) and antigenically distinct
 856 (B/Florida/4/2006, FL06) B/Yamagata influenza viruses were determined 14 days post second
 857 immunization by micro-neutralization assays. Data are presented as geometric means \pm 95% CI (n
 858 = 5 or 6). C. BALB/c mice were vaccinated i.m. with the FLUCOV-10, monovalent BA.2.75.2
 859 mRNA vaccines derived from FLUCOV-10 or a placebo. Neutralizing antibody titers against
 860 vaccine matched (BA.2.75.2) and antigenically distinct (BA.5.2) SARS-CoV-2 viruses were
 861 determined 14 days post second immunization by micro-neutralization assays. ns,
 862 non-significant; *, $p < 0.05$; **, $p < 0.01$.

863



864

865 **Supplemental Figure 2. Survival Rates in Mice Immunized with FLUCOV-10 and**
866 **Challenged with Influenza or SARS-CoV-2 Viruses (related to Figure 4).**

867 The mice were challenged 3 weeks post second immunization with indicated viruses and the
868 survival rates were monitored for 7 or 14 days.

869

870